FILTER BANKS IN DIGITAL COMMUNICATIONS

P. P. Vaidyanathan

Dept. of Electrical Engineering, California Institute of Technology, Pasadena, CA.

Contact Author: P. P. Vaidyanathan, Dept. Electrical Engr., 136-93, California Institute of Technology, Pasadena, CA 91125. Ph:(626) 395 4681. Email: ppvnath@sys.caltech.edu

Abstract. Digital signal processing has played a key role in the development of telecommunication systems over the last two decades. In recent years digital filter banks have been occupying an increasingly important role in both wireless and wireline communication systems. In this paper we review some of these applications of filter banks with special emphasis on discrete multitone modulation which has had an impact on high speed data communication over the twisted pair telephone line. We also review filter bank precoders which have been shown to be important for channel equalization applications.[1]

1. INTRODUCTION

Efficient and successful communication of messages via imperfect channels is one of the major triumphs of information technology today. With more and more users desiring to share communication channels, the importance of clever exploitation of the bandwidth becomes paramount. For example telephone lines (twisted-pair channels) which were originally intended to carry speech signals (about 4 kHz bandwidth) are today used to carry several megabits of data per second. This has been possible because of efficient use of high frequency regions which suffer from a great deal of line attenuation and noise. As a result of these developments the twisted pair telephone line, which reaches nearly every home and office in the western world, can today handle high speed internet traffic as exemplified by popular services such as the DSL (digital subscriber loop), ADSL, and so forth. As someone pointed out, *twisted pair copper lines are buried but not dead,* thanks to advanced signal processing technology!

Communication channels can be wireless or wireline channels, or a combination of both. In any case they introduce linear and nonlinear distortions, random noise components, and deterministic interference. The transmission of information with high rate and reliability under such unfavorable conditions has been possible because of fundamental contributions from many disciplines such as information theory, signal processing, linear system theory, and mathematics.

The role of digital signal processing in communication systems has been quite significant [17,18,6]. In

[1]Work supported in parts by the NSF grant MIP 0703755 and ONR grant N00014-99-1-1002.

this paper we emphasize some of these, especially the role of filter banks. The aim here is to give an overview of filter banks as applied to digital communication systems. Filter banks were originally proposed for application in speech compression more than 25 years ago (see references in [7]). Today they are used for the compression of image, video, and audio signals, and the story of their success can be found in many references. More recently filter banks have been used in digital communication systems in many forms. Some of these include perfect digital transmultiplexing [26, 1], filter-bank precoding for channel equalization [29, 15], equalization with fractionally spaced sampling [28], and discrete multitone modulation [18, 21, 23]. Filter banks have been used in high speed DSL services for internet traffic [6]. They have also been considered for blind equalization in wireless channels [8, 16].

2. THE NOISY CHANNEL

In this paper we model the communication channel as a linear time invariant system with transfer function $C(z)$ followed by an additive Gaussian noise source $e(n)$ as shown in Fig. 1. In a digital communication system each sample $x(n)$ comes from a fixed finite set of values. This set of values is called a constellation, some standard examples being PAM and QAM constellations explained in Fig. 2. If each symbol $x(n)$ is a b-bit number and there are f_s symbols per second, then the **bit rate** is $\mathcal{R} = bf_s$ bits per second. For example if $f_s = 1$ MHz and $b = 4$ then $\mathcal{R} = 4$ megabits per second (Mbps).

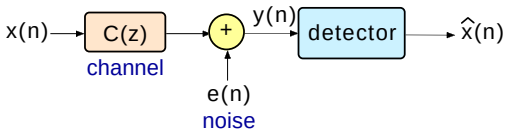

Fig. 1. A simple model for a digital communication system. Here a sequence of symbols $x(n)$ is transmitted through a channel with transfer function $C(z)$ and additive noise $e(n)$.

The received signal $y(n)$ is a noisy and distorted version of $x(n)$. The detector at the receiver has to guess the value of $x(n)$ based on $y(n)$. The estimated value $\widehat{x}(n)$ belongs to the same constellation that $x(n)$ came from. If $x(n) = \widehat{x}(n)$ there is no error; otherwise the detection is erroneous. In practice there is a nonzero **probability of error** $\mathcal{P}_e$ in this detection because of the noise $e(n)$ and the intersymbol interference caused by the channel $C(z)$. The acceptable value of $\mathcal{P}_e$ depends on application. For example it is in the range 10^{-7} to 10^{-9} for DSL applications; for digital speech with mobile phone quality, larger $\mathcal{P}_e$ is acceptable whereas for deep space communication, $\mathcal{P}_e$ has to be quite a bit smaller.

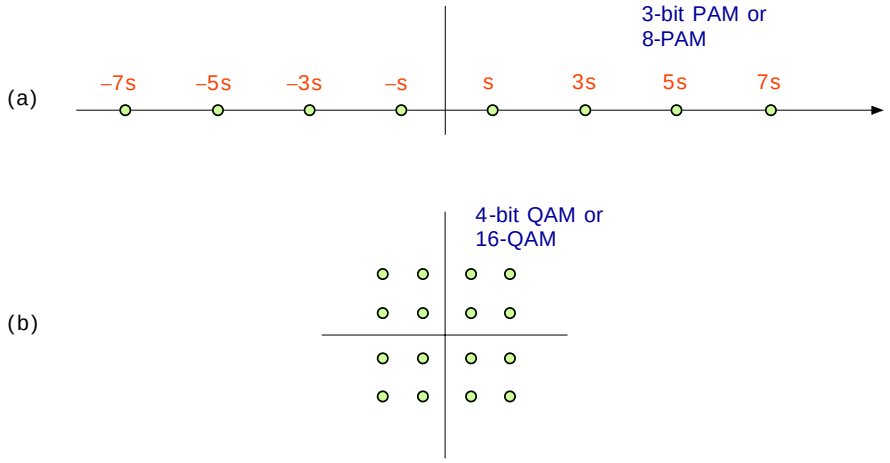

Fig. 2. (a) For the case of Pulse Amplitude Modulation (PAM), the sample $x(n)$ is a quantized real number as demonstrated in part (a) for 3-bit PAM (also called 8-PAM). (b) For the case of Quadrature Amplitued Modulation (QAM) $x(n)$ can be regarded as a compex number, taking one of 2^b possible values from a rectangular constellation as demonstrated in part (b) for $b = 4$ bits (called 16-QAM). More efficient constellations exist [14]. The distance between the constellation words (e.g., s in part (a)) can be controlled to control the transmitted power.

The model shown in Fig. 1 does not work in all situations. For example, mobile phone channels are time varying because of vehicular movement, and a single $C(z)$ cannot be used to represent them successfully. However a number of practical channels (e.g., the wireline telephone channel) can be approximated by this. A second remark is that the figure implicitly uses discrete time notations. In practice, the sequence $x(n)$ is converted into a continuous time pulse train $\sum_n x(n)p(t - nT)$ before imposing it on the channel. The output of the channel is sampled and digitized to obtain $y(n)$. These details are not shown in the figure. It should be understood that $C(z)$ and $e(n)$ are the effective discrete time equivalents of the actual channel parameters.

3. POWER ALLOCATION AND WATER-FILLING STRATEGY

The transmitted signal **power** P is proportional to the mean square value of $x(n)$. Assume that $x(n)$ is a wide sense stationary random process [14]. Then the power is the integral of the power spectrum $S_{xx}(e^{j\omega})$, that is, $P = \int_0^{2\pi} S_{xx}(e^{j\omega})d\omega/2\pi$. For a given channel the average probability of error $\mathcal{P}_e$ at the receiver depends on the transmitted power P, and the bit rate $\mathcal{R}$. We can decrease the error probability by transmitting more power. For fixed power, the error probability increases with bit rate $\mathcal{R}$.

Note that the power spectrum of $x(n)$ tells us how its **power is distributed** in frequency. By carefully shaping it, we can increase the achievable rate (for fixed error probability and trasmitted power). The idea is to "pour" more power in the regions where the channel gain is large and noise spectrum is small. This can be pursued in a mathematically rigorous way using fundamentals from information theory [14].

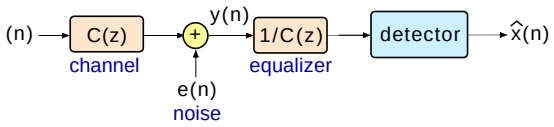

Fig. 3. A channel, equalized with an ideal equalizer $1/C(z)$ (also called the zero-forcing equalizer). The effective noise $q(n)$ as seen by the detector is nothing but $e(n)$ filtered through $1/C(z)$.

If the transfer function of the channel is known, then the detector can equalize it by using the filter $1/C(z)$. This is called the ideal equalizer. It is also known as the **zero-forcing** equalizer for reasons explained in [14]. In practice $1/C(z)$ can be approximated with a stable (possibly FIR) filter. As seen from Fig. 3, the effective noise $q(n)$ seen by the receiver is $e(n)$ filtered through $1/C(z)$. This has the power spectrum

$$S_{qq}(e^{j\omega}) \triangleq \frac{S_{ee}(e^{j\omega})}{|C(e^{j\omega})|^2} \qquad \text{(effective noise power spectrum)}. \tag{1}$$

This ratio summarizes the channel completely for the purpose under discussion. If $C(z)$ has zeros close to the unit circle, then $1/C(z)$ has poles near the unit circle and the noise gain can be large. In frequency regions where the ratio $S_{qq}(e^{j\omega})$ is small, we should allocate more power. In fact the optimal power distribution $S_{xx}(e^{j\omega})$ can be described precisely with the help of Fig. 4. This figure says that

$$S_{xx}(e^{j\omega}) = \begin{cases} \lambda - S_{qq}(e^{j\omega}) & \text{when this is nonnegative} \\ 0 & \text{otherwise,} \end{cases} \tag{2}$$

where λ is a constant. That is, the transmitted power at a frequency should be equal to the gap between λ and $S_{qq}(e^{j\omega})$. Notice that in regions where the channel is "too bad" ($S_{qq}(e^{j\omega}) > \lambda$) we transmit no power at all. If we imagine a bowl with its bottom shaped like $S_{qq}(e^{j\omega})$, then $S_{xx}(e^{j\omega})$ is the height of water filling the bowl, with λ denoting the uniform water level everywhere. This is a classic result on power allocation, and is called the **water filling** rule [14]. It is clear that the area under $S_{xx}(e^{j\omega})$ (total power) increases with choice of λ. The choice of λ therefore depends on the total available power P.

For fixed total power P and fixed channel, the **capacity** $\mathcal{C}$ is the maximum rate at which information can be transmitted with arbitrarily small error probability. This should not be confused with the actual bit rate $\mathcal{R}$ with nonzero error probality $\mathcal{P}_e$. Evidently if $\mathcal{P}_e$ is allowed to be large enough then $\mathcal{R}$ can be made larger than the capacity $\mathcal{C}$. In situations where $\mathcal{P}_e$ is required to be reasonably small, $\mathcal{C}$ can be regarded as a useful bound on acheivable rate $\mathcal{R}$.

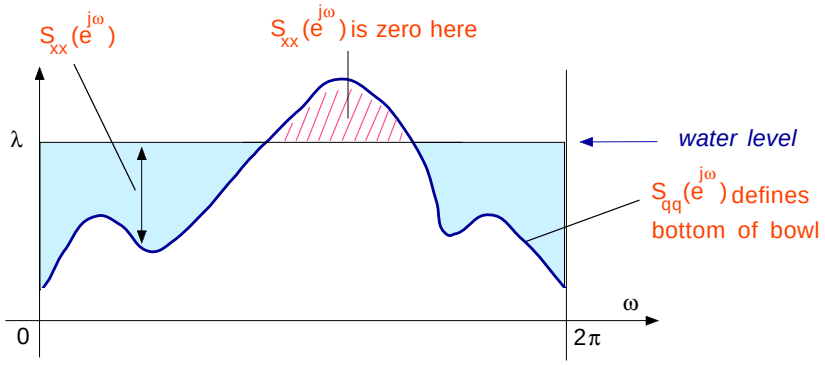

Fig. 4. Relation between the input power spectrum $S_{xx}(e^{j\omega})$ and the effective noise power spectrum $S_{qq}(e^{j\omega})$ to achieve maximum rate for fixed total power. This is called the water filling rule.

How do we shape the power spectrum $S_{xx}(e^{j\omega})$ to satisfy the water-filling type of power allocation? This is tricky because we do not have a great deal of freedom to shape things, especially if $x(n)$ is user generated data! For example $x(n)$ could be binary data or data from a PAM or QAM constellation, and might behave like an iid (independent identically distributed) sequence with a practically flat power spectrum. A clever way to approximate optimal power allocation would be to divide the channel bandwidth into several subbands and transmit in each subband channel separately [4,9]. This already suggests a resemblance to frequency division multiplexing but the main difference now is that the different subband channels carry different parts of a single input stream. How this is actually accomplished will be explained in Sec. 6.

4. DECIMATORS, EXPANDERS, AND MULTIPLEXERS

Before proceeding further we review a few standard building blocks and terminology used in multirate signal processing. Most of the details can be found in [22]. The building blocks $\uparrow M$ and $\downarrow M$, shown in Fig. 5 are called the expander and decimator respectively. Their operation is explained in the figure caption.

Two standard operations called "blocking" and "interleaving" often arise in communication systems that use filter banks. It is sometimes convenient to explain these using multirate building blocks. These are shown in Figs. 6(a) and 6(b). The connection between the signal $v(n)$ and the "blocked components" $v_k(n)$ is indicated in Fig. 6(c) using the example of $M = 3$. It is clear that we can regard $v(n)$ as a **time-domain multiplexed** or **TDM** version of the individual signals $v_k(n)$. The components $v_k(n)$ are also called the **polyphase** components of $v(n)$ with respect to M [22].

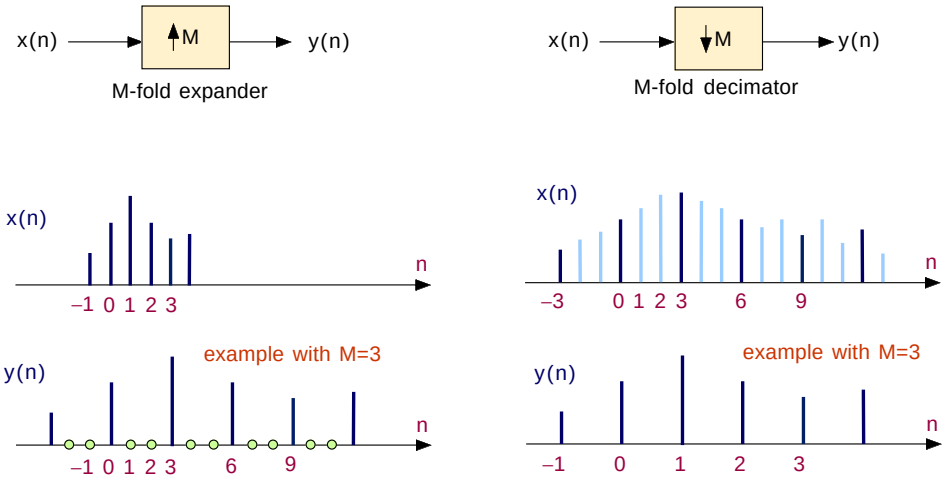

Fig. 5. The M-fold expander merely inserts $M-1$ zeros between adjacent samples, as demonstrated in the figure for $M=3$. The M-fold decimator has input-output relation $y(n)=x(Mn)$. Thus, only a subset of input samples are retained. This is demonstrated in the figure for $M=3$. Note that the samples automatically get renumbered so that $y(1)=x(M), y(2)=x(2M)$ and so forth.

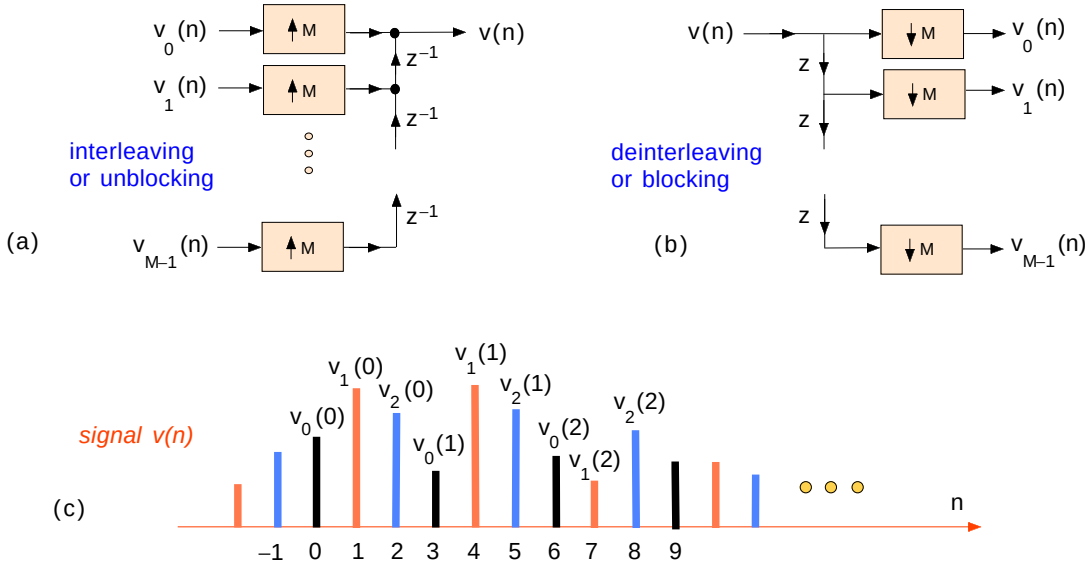

Fig. 6. (a), (b) The operations of interleaving and deinterleaving using multirate building block notation. (c) Demonstration for $M=3$. The interleaving operation is also called unblocking. Similarly deinterleaving is also called blocking.

5. THE DIGITAL TRANSMULTIPLEXER

Our next step would be to describe the operation of a filter bank structure called the transmultiplexer [12,26,22]. It was originally intended to convert data between time division multiplexed (TDM) format and frequency division multiplexed (FDM) format. Figure 7(a) shows a schematic of this in all-discrete language.

Here $F_k(z)$ are called transmitting filters or interpolation filters.

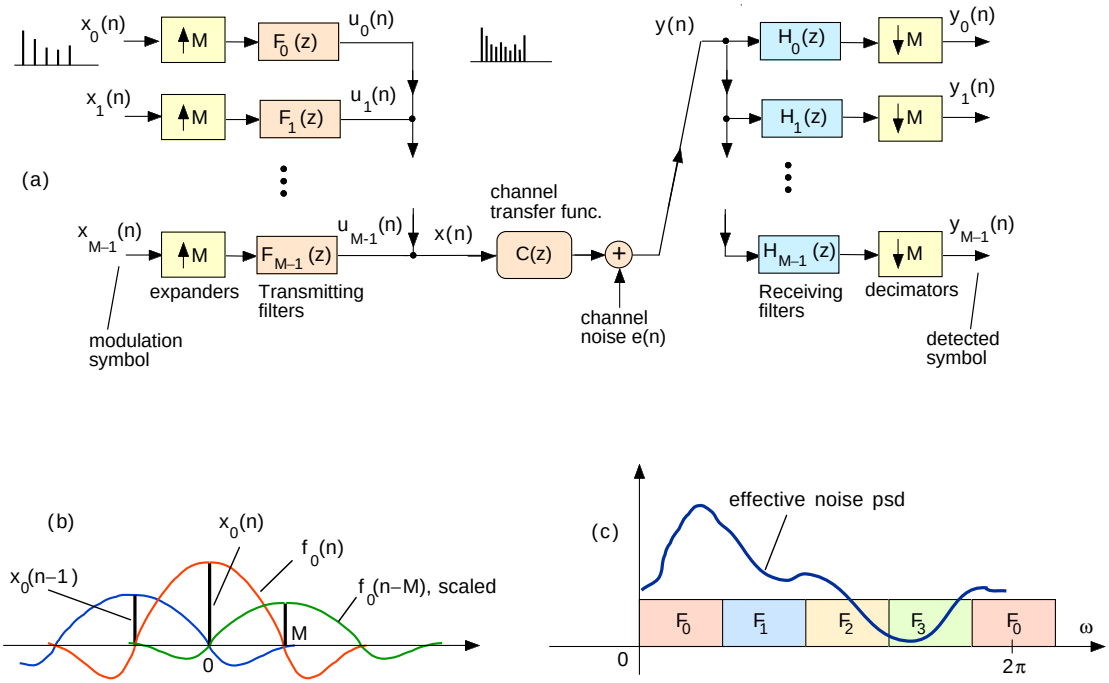

Fig. 7. (a) The digital transmultiplexer, (b) operation of the interpolation filter $F_0(z)$, and (c) frequency responses of the transmitting filters (assumed to be ideal infinite order filters). Only the envelope of the samples of $f_0(n)$ are shown in (b).

The kth transmitting filter has output

$$u_k(n) = \sum_{i=-\infty}^{\infty} x_k(i) f_k(n - iM). \tag{3}$$

Figure 7(b) demonstrates how this construction is done for the 0th filter $F_0(z)$, assumed to be lowpass. Essentially we draw one copy of the impulse response sequence $f_0(.)$ around every sample of $x_0(n)$ (separated by M) and add them up. Thus $u_k(n)$ is an interpolated version of $x_k(n)$ and has M times higher rate. The outputs of the filters $F_1(z), F_2(z)$ and so forth are more complicated waveforms because they are bandpass. The filters $\{F_k(e^{j\omega})\}$ traditionally cover different uniform regions of frequency as shown in Fig. 7(c). The signals $u_k(n)$ are analogous to modulated versions of the "baseband" sequence $x_k(n)$ because the bandwidth is shifted to the passband of $F_k(z)$. These are packed into M adjacent frequency bands (passbands of the filters) and added to obtain the composite signal $x(n)$. With the filters $F_k(z)$ chosen as good bandpass filters, we can regard $x(n)$ as a **frequency division multiplexed** or **FDM** version of the separate signals $x_k(n)$. By contrast, if $F_k(z)$ are just delay elements z^{-k}, then the transmitter part is similar to Fig. 6(a) and $x(n)$

is a time-multiplexed version of the M signals $x_k(n)$. Letting T denote the spacing between samples of $x(n)$, we see that the samples of $x_k(n)$ for any given k are separated by a longer duration of MT seconds.

The receiving filter bank $\{H_k(z)\}$ separates the signal $y(n)$ into the components $y_k(n)$ which are distorted and noisy versions of the symbols $x_k(n)$. The task at this point is to detect the symbols $x_k(n)$ from $y_k(n)$ with acceptable error probability. Thus, even though $x_k(n)$ is interpolated to get $u_k(n)$, it is not necessary to ensure $u_k(Mn) = x_k(n)$; the crucial issue is to make $y_k(n)$ resemble $x_k(n)$.

6. DISCRETE MULTITONE MODULATION (DMT)

The transmultiplexer configuration is used in another scheme called **discrete multitone modulation** or DMT scheme. The main difference is in the interpretation of the signals $x(n)$ and $x_k(n)$. To explain this consider Fig. 8(a) which shows the first stage of multitone modulation [4] called the **parsing stage**. Here $s(n)$ represents **binary data** to be transmitted over a channel. This data is divided into nonoverlapping b-bit blocks. The b bits in each block are partitioned into M groups, the kth group being a collection of b_k bits (demonstrated in the figure for $M = 3$). Thus the total number of bits b per block can be expressed as

$$b = \sum_{k=0}^{M-1} b_k \tag{4}$$

The b_k bits in the kth group constitute the kth symbol x_k which can therefore be regarded as a b_k-bit number. For the nth block, this symbol is denoted as $x_k(n)$. This is the **modulation symbol** for the kth band. The collection of symbols $\{x_0(n),\ x_1(n),\ \ldots\ , x_{M-1}(n)\}$ is together referred to as the **DMT symbol**. The sample $x_k(n)$ is typically a PAM or a QAM symbol (Fig. 2). The transmitting filters $f_k(n)$ create the M-fold higher rate signals $u_k(n)$ as before, which are then added to produce the composite signal $x(n)$. In this way, various parts of the original binary message $s(n)$ are packed into different frequency regions allowed by the channel [4, 9].

Notice that for a given constellation, the power can be increased or decreased by scaling the distance between the codewords (e.g., by adjusting s for the PAM constellation in Fig. 2(a)). We therefore have the freedom to allocate different powers for different subband channels. In this way the classical **water-filling rule can be approximated**. For a given transmitted power and probability of error, multitone modulation yields better bit rate than single tone modulation ($M = 1$ case), assuming no channel coding.

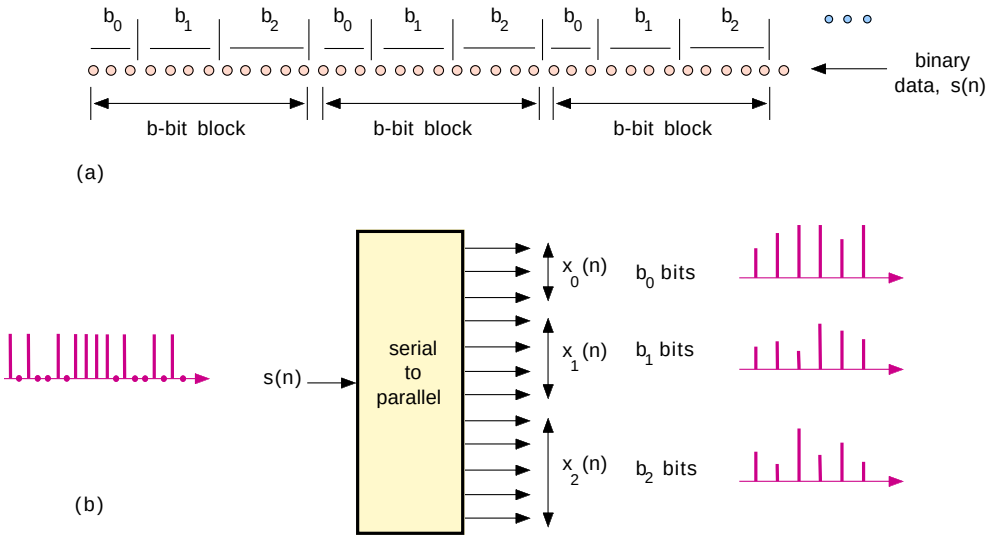

Fig. 8. Parsing stage in discrete multitone (DMT) modulation. A binary stream $s(n)$ is subdivided into b-bit blocks and each block is subdivided into M subgroups. The kth subgroup defines a b_k-bit symbol $x_k(n)$. Note that $x_k(n)$ and $x_k(n+1)$ are separated by bT seconds if $s(n)$ and $s(n+1)$ are separated by T seconds.

Background material on the DMT system and more generally on the use of digital filter banks in communications can be found in [1,5,9,21]. The DMT idea is similar in principle to **subband coding** [7, 27, 22] where a signal $x(n)$ to be quantized is first decomposed into subbands.

7. BIORTHOGONALITY AND PERFECT DMT SYSTEMS

Consider a linear time invariant system with impulse response $h(n)$ and transfer function $H(z)$ sandwiched between an expander and decimator (Fig. 9(a)). It can be shown that this is equivalent to a linear time invariant system with decimated impulse response $g(n) = h(Mn)$. In z-transform notation we denote this as $G(z) = [H(z)]_{\downarrow M}$.

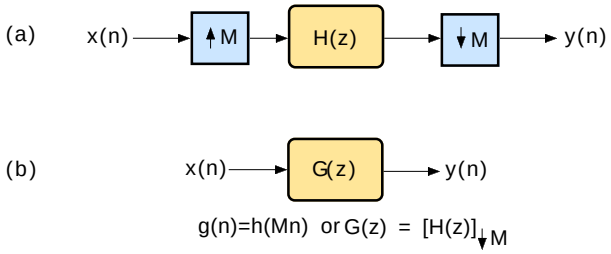

Fig. 9. A transfer function $H(z)$ sandwiched between an expander and a decimator is equivalent to another transfer function $G(z)$ with impulse response $g(n) = h(Mn)$.

Using this simple idea, we can understand the operation of the DMT system in a very effective way. Thus the transfer function $D_{km}(z)$ from $x_m(.)$ to $y_k(.)$ in Fig. 7(a) is the decimated version of the product-filter

$H_k(z)C(z)F_m(z)$. If this is nonzero for $m \neq k$ then the symbol $y_k(n)$ is affected by $x_m(i)$ resulting in **interband** interference. Similarly if $D_{kk}(z)$ is not a constant then $y_k(n)$ is affected by $x_k(i), i \neq n$, due to the filtering effect of $D_{kk}(z)$. This is called **intraband** interference. If interband and intraband interferences are eliminated, the DMT system is said to be free from **intersymbol** interference (ISI). If we assume that the filters are ideal nonoverlapping bandpass filters stacked as in Fig. 7(c), then there is no interband interference. Furthermore, suppose that $C(z)$ is completely equalized with the inverse filter $1/C(z)$ as shown in Fig. 10. Then the system is ISI free, and $y_k(n) = x_k(n)$ for all k (in absence of noise), and we have the perfect symbol recovery or **PR** property.

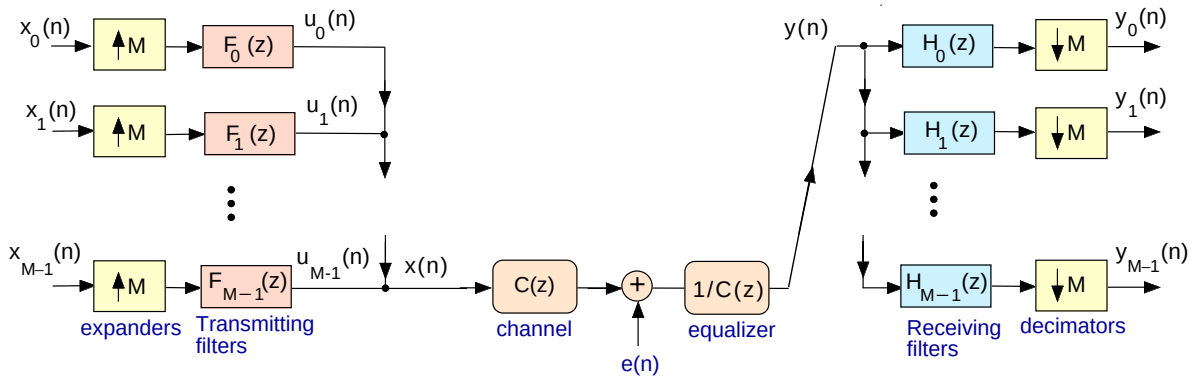

Fig. 10. The DMT system with ideal channel equalizer $1/C(z)$. This system has the perfect symbol recovery (PR) property in absence of noise if the filter bank $\{H_k, F_m\}$ is biorthogonal. See text.

Ideal nonoverlapping filters are of course unrealizable, and good approximations of such filters are expensive. It turns out that perfect symbol recovery can be obtained even with non ideal filters having overlapping responses. This idea goes back to early work on transmultiplexers [26] and is related to the notion of a biorthogonal filter bank. To explain this, consider what happens when the channel introduces no distortion ($C(z) = 1$). Under this condition we have perfect symbol recovery if and only if the transmitting and receiving filters satisfy the **biorthogonality property** defined as

$$H_k(z)F_m(z)\Big|_{\downarrow M} = \delta(k-m) \qquad \text{(biorthogonality)}. \tag{5}$$

This means that the impulse response $g_{km}(n)$ of the product filter $G_{km}(z) \triangleq H_k(z)F_m(z)$ has the **Nyquist(M)** or zero-crossing property

$$g_{km}(Mn) = 0 \tag{6}$$

for $k \neq m$ and $g_{kk}(Mn) = \delta(n)$ as demonstrated in Fig. 11 for $M = 3$. This condition is readily achieved with careful design of filters. For example, it is possile to design FIR biorthogonal filter banks with almost any filter length.

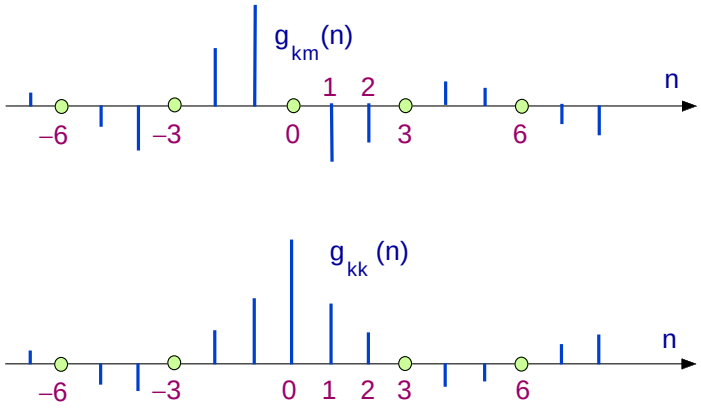

Fig. 11. In a biorthogonal transmultiplexer, we have the perfect symbol recovery property in absence of channel distortion $C(z)$ and channel noise $e(n)$. This is achieved by constraining the filters such that the products $G_{km}(z)$ have the Nyquist(M) property. That is, their impulse responses have the zero crossing property at integer multiples of M as demonstrated above for $M = 3$.

In this paper we shall make the simplifying assumption that $\{F_m, H_k\}$ is biorthogonal (i.e., Eq. (5) holds) and that the channel transfer function $C(z)$ is equalized by using the inverse filter or zero-forcing equalizer $1/C(z)$ just before entering the bank of filters $\{H_k(z)\}$. In a biorthogonal DMT system with zero-forcing equalizer, the only remaining distortion is due to the channel noise. The received symbol can be written as

$$y_k(n) = x_k(n) + q_k(n) \tag{7}$$

where $q_k(n)$ is the channel noise filtered through $H_k(z)/C(z)$ and decimated (Fig. 12(a)). Thus the variance of $q_k(n)$ can be calculated using the equivalent circuit shown in Fig. 12(b) where $S_{qq}(e^{j\omega}) = S_{ee}(e^{j\omega})/|C(e^{j\omega})|^2$ is the equivalent noise spectrum defined in Sec. 3. This figure shows an **analysis bank** $\{H_k(z)\}$ whose input is a noise source with effective power spectrum given by (1).

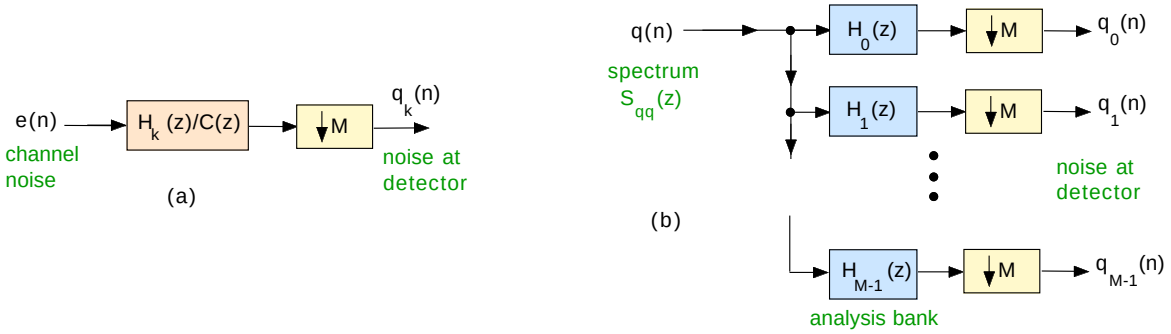

Fig. 12. (a) The effect of the channel noise at the detector inputs can be modelled as the filtered version of the channel noise. (b) The noise variances at the detector inputs can therefore be calculated as the subband variances in a maximally decimated analysis filter bank, whose input has the power spectrum $S_{qq}(e^{j\omega}) = S_{ee}(e^{j\omega})/|C(e^{j\omega})|^2$.

8. OPTIMIZATION OF DMT FILTER BANKS

In this section we discuss the optimization of filter banks used in DMT systems. The variance of the symbol $x_k(n)$ in Fig. 7(a) represents its **average power** P_k. For simplicity assume that $x_k(n)$ comes from a b_k-bit PAM constellation (Fig. 2) with equal probability for all codewords. Assume further that the noise $q_k(n)$ is Gaussian with variance $\sigma_{q_k}^2$. Then the **probability of error** in detecting $x_k(n)$ can be expressed in terms of the signal power P_k, noise variance $\sigma_{q_k}^2$, and number of bits b_k. The exact expression can be found in many references (e.g., see [14], [23], [24]). The main point is that this expression can be inverted to obtain the total power in the symbols $x_k(n)$. The result takes the form [23–24]

$$P = \sum_{k=0}^{M-1} P_k = \sum_{k=0}^{M-1} \beta\Big(\mathcal{P}_e(k), b_k\Big) \times \sigma_{q_k}^2 \tag{8}$$

where the exact nature of the function $\beta(.,.)$ is not of immediate interest. This expression says that if the acceptable probabilities of error at the bit rates $\{b_k\}$ are $\{\mathcal{P}_e(k)\}$, then the total power P has to be at least as large as the right hand side of (8). If we try to decrease $\mathcal{P}_e(k)$ for a given bit rate, we need more power.

The crucial point to note here is that the power P can be minimized by carefully controlling the variances $\sigma_{q_k}^2$ of the noise components $q_k(n)$ at the detector inputs. Given the channel $C(z)$ and the channel noise spectrum $S_{ee}(z)$, the only freedom we have in order to control $\sigma_{q_k}^2$ is the choice of the filters $H_k(z)$ (see Fig. 12(b)). But we have to control these filters under the constraint that $\{H_k, F_m\}$ is biorthogonal. Since the scaled system $\{\alpha_k H_k, F_m/\alpha_m\}$ is also biorthogonal (as we can show using (5)), it appears that the variances $\sigma_{q_k}^2$ can be made arbitrarily small by making α_k small. The catch is that the transmitting filters $F_m(z)/\alpha_m$ will have correspondingly larger energy which means an increase in the power actually fed into the channel. One correct approach to do the optimization would be to impose a **power constraint**. Mathematically this is trickier than constraining the powers P_k in the symbols $x_k(n)$. In the next section we confine the optimization to a class of filter banks called orthonormal filter banks. In this case the optimization problem is especially easy to formulate, and elegant solutions can be found as well.

9. ORTHONORMAL DMT SYSTEMS

Recall from Fig. 7(a) that the subband channel signals $u_k(n)$ are the outputs of interpolation filters, and can be expressed as in Eq. (3). We can regard the subchannel signal $u_k(n)$ as belonging to a subspace spanned by the basis functions

$$\ldots f_k(n+M),\ f_k(n),\ f_k(n-M),\ f_k(n-2M)\ldots \tag{9}$$

covering the kth frequency band. The basis has infinite number of elements, each element being a filter obtained from the preceding element by a time-shift of M samples. The composite signal $x(n)$ which enters

the channel is therefore a linear combination of the basis functions from all the channels. We say that a set of M filters $\{F_k(z)\}$ is orthonormal if these basis functions are orthogonal to each other, and each of them is normalized to have unit energy. For perfect symbol recovery (or biorthogonality), the transmitting and receiving filters in any orthonormal filter bank are related by

$$h_k(n) = f_k^*(-n) \tag{10}$$

which is called **time reversed-conjugation**. This condition means in particular that the transmitting and receiving filters have identical frequency response magnitudes. Orthonormal filter banks have been extensively studied and documented, see for example [22], [27] and references therein. It is possible to have orthonormal filter banks where the filters are FIR. An example is the filter bank where $f_0(n)$ is chosen as a rectangular pulse of length M and $f_k(n)$ are the modulated versions

$$f_k(n) = f_0(n)e^{j\omega_k n} \tag{11}$$

with $\omega_k = 2\pi k/M$ representing the kth center-frequency. See Fig. 13. The frequency responses are uniformly shifted versions of $F_0(e^{j\omega})$ as shown in the figure.

This is called the DFT filter bank because it can be implemented with a DFT matrix and an inverse DFT (IDFT) matrix as shown in Fig. 14. At each instant of time n, the DMT symbol $\{x_0(n), x_1(n), \ldots x_{M-1}(n)\}$ is transformed into the IDFT domain. The components $v_k(n)$ of the resulting symbol are interleaved to obtain the channel signal $x(n)$. At the receiver the signal is de-interleaved and a DFT is performed. The results $y_k(n)$ are noisy versions of the transmitted symbols $x_k(n)$. Orthonormality of the basis functions in (9) follows from the fact that the DFT matrix (with proper normalization) is unitary. The DFT filter bank is used widely in DMT systems [5] for certain types of DSL services.

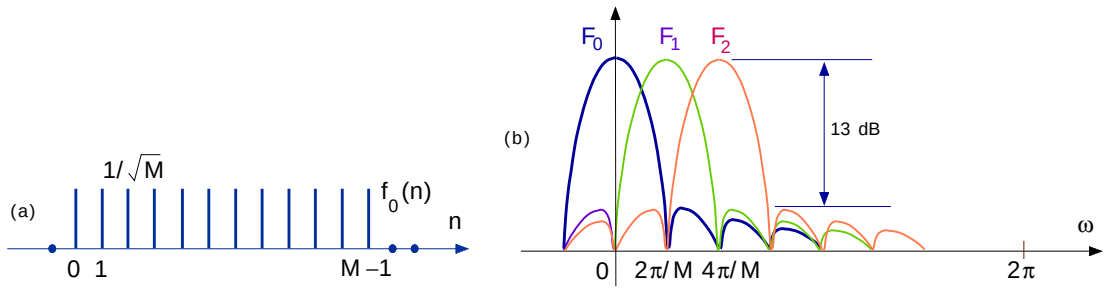

Fig. 13. An example of the uniform DFT filter bank. (a) Impulse response of $F_0(z)$ and (b) magnitude responses of the digital filters $F_k(e^{j\omega})$. Each filter response is a frequency-shifted version of the preceding filter. The shifts are in uniform increments of $2\pi/M$ where M is the number of filters. If the peak passband response is normalized to 0 dB, the minimum stop band attenuation is about -13 dB.

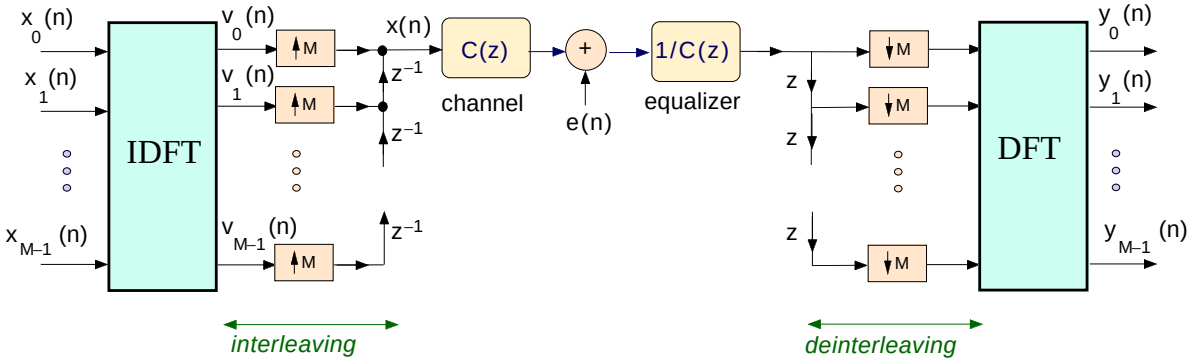

Fig. 14. DMT system based on the uniform DFT filter bank. The channel equalizer $1/C(z)$ can be approximated well in many ways. An indirect but effective way to perform equalization is to introduce redundancies such as the cyclic prefix [13].

The popularity of the DFT based DMT filter bank arises from the fact that if M is chosen as a power of two (e.g., $M = 512$ which is typical) the DFT can be implemented very efficiently using the fast Fourier transform (FFT) algorithm. By using bit allocation in the transform domain, the DFT based DMT system can take advantage of the shape of the effective noise spectrum (1) and obtain a performance close to the water-filling ideal (Sec. 3). In Sec. 10.3 we shall provide numerical examples in terms of bit rates and transmitted power.

10. OPTIMAL ORTHONORMAL DMT SYSTEMS

In an orthonormal DMT filter bank the transmitting and receiving filters have unit energy. So we cannot insert arbitrary scale factors in front of $H_k(z)$ to reduce the noise at the detector input. Moreover, orthonormality also implies that the average variance of the composite signal $x(n)$ is the average of the variances of the symbols $x_k(n)$. That is, the actual power entering the channel is proportional to the sum of powers P_k in the symbols $x_k(n)$. Refer again to Fig. 12(b) now. For a given channel the effective noise spectrum $S_{qq}(e^{j\omega})$ is fixed (ratio defined in (1)). Assume further that the integer M (number of subchannels) is fixed. For a given set of error probabilities and bit rates, the required transmitted power depends only on the noise variances $\sigma_{q_k}^2$ as shown by Eq. (8). We have to find an orthonormal filter bank such that this power is minimized. This is the problem of designing an optimal orthonormal DMT system. It turns out that the solution $\{H_k\}$ depends only on the effective noise spectrum and not on the desired values of error probabilities and bit rates.

10.1. KLT Based DMT Systems

Consider for example the class of FIR orthonormal DMT systems, that is, systems where $F_k(z)$ and $H_k(z)$ are FIR. Assume further that the filter lengths are constrained to be no larger than M. An example is the

DFT based DMT system described in Sec. 9 with transmitting filters as in (11). In view of the time-reveresed conjugation property (10), the receiving filters are given by

$$h_k(n) = \begin{cases} e^{j\omega_k n}/\sqrt{M} & \text{for } -(M-1) \le n \le 0, \\ 0 & \text{otherwise.} \end{cases}$$

Since the channel noise is filtered by the DFT matrix, the noise model for this system can be drawn as in Fig. 15 where **T** represents the DFT matrix. This is precisely the structure of the noise model of Fig. 12(b), drawn in a different way. In general any pair of receiver noise components $q_k(n)$ and $q_m(n)$ have some statistical correlation between them. But it is possible to replace the DFT matrix with another unitary matrix **T** such that $q_k(n)$ and $q_m(n)$ are uncorrelated for all n when $k \neq m$. Such a decorrelating matrix **T** depends only on the power spectrum of the effective noise $q(n)$. It is called the $M \times M$ KLT matrix for $q(n)$. Essentially it is a unitary matrix which diagonalizes the $M \times M$ autocorrelation matrix of $q(n)$. It can be shown that if **T** is chosen as the KLT matrix (and its inverse used in the transmitter) then the **required power P is minimized**. The KLT offers the optimal DMT solution if we compare all orthonormal DMT systems with FIR filters of length $\le M$. The proof follows as a special case of the results in [23,24].

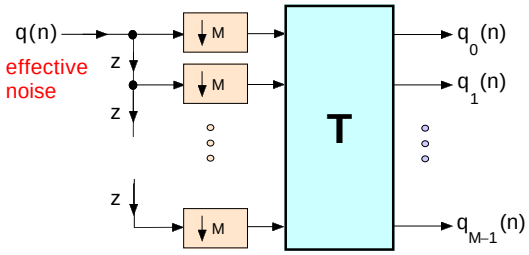

Fig. 15. Noise model for the DMT filter bank, redrawn in terms of the transform matrix **T**. If **T** is the DFT matrix, then this is the noise model for the DFT based DMT. If **T** is the KLT matrix for the effective noise $q(n)$ then this corresponds to an optimal DMT system. See text.

10.2. Optimal Orthonormal DMT Systems Using Unconstrained Filters

If the transmitting and receiving filters are allowed to have infinite length with no causality restrictions, then nonoverlapping brickwall filters are allowed. In fact ideal filters with multiple passbands are allowed as well and could be useful as we shall see later. Assuming orthonormality, the transmitting filters are constrained as $F_k(e^{j\omega}) = H_k^*(e^{j\omega})$. What is the best choice of the frequency responses of the receiving filters $\{H_k(z)\}$ if we wish to minimize transmitted power? The answer again depends only on the effective noise spectrum $S_{qq}(e^{j\omega})$. In fact the optimal choice of $\{H_k(z)\}$ is the so-called **principal component** filter bank or **PCFB** for the power spectrum $S_{qq}(e^{j\omega})$, as shown in [23,24].

To explain what a PCFB is, assume that we are given a class $\mathcal{C}$ of M channel orthonormal analysis filter

banks as in Fig. 12(b). Given an input power spectrum $S_{qq}(e^{j\omega})$, a PCFB in $\mathcal{C}$ is a filter bank such that the output variances $\{\sigma_{q_k}^2\}$, arranged in nonincreasing order $\sigma_{q_k}^2 \geq \sigma_{q_{k+1}}^2$ have a very special property. Namely, the partial sums of these variances,

$$\sigma_{q_0}^2, \quad \sigma_{q_0}^2 + \sigma_{q_1}^2, \quad \sigma_{q_0}^2 + \sigma_{q_1}^2 + \sigma_{q_2}^2, \ \ldots \tag{12}$$

are larger than the corresponding partial sums for any other filter bank in this class.[2] This idea is demonstrated in Fig. 16. If $\mathcal{C}$ is the class of orthonormal filter banks with filter length $\leq M$ then the KLT of the input is a PCFB. If $\mathcal{C}$ represents the class of ideal orthonormal filter banks (with filters allowed to be noncausal with unrestricted lengths) then there is a systematic way to construct the PCFB [24]. Unlike the brickwall filter bank of Fig. 7(c), each filter can have multiple passbands. Thus, the PCFB partitions the frequency domain in a different way according to the nature of the input spectrum.

For an arbitrary class $\mathcal{C}$ such as the class of FIR orthonormal filter banks with length constrained by some integer, the PCFB may not in general exist. The detailed theory of the PCFB is available in [2], and a tutorial review can be found in [24].

Assume that the error probabilities and total allowed power are fixed. It can then be shown that the **bit rate**, which is proportional to $\sum_k b_k$, is maximized by the PCFB. Similarly, with appropriate theoretical modelling the **information capacity** (for fixed total power) is also maximized by the PCFB. Details can be found in [3], [23], [25].

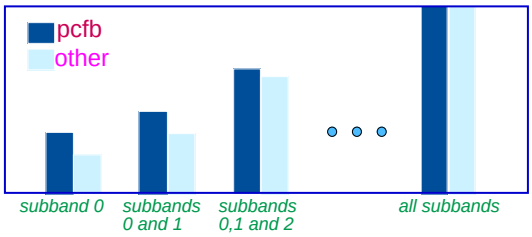

Fig. 16. This figure schematically explains what a principal component filter bank (PCFB) does. The dark blue columns represent the partial sums of subband variances of a PCFB in a class $\mathcal{C}$ of orthonormal filter banks, and the light blue columns represent the same sums for an arbitrary filter bank in $\mathcal{C}$. By definition, the PCFB partial sums always dominate. Remember here that the sum of *all subband variances* is the same for all orthonormal filter banks, and is equal to M times the input variance.

10.3. Examples

Assume that the effective noise power spectrum has the hypothetical form shown in Fig. 17(a). We have shown only the region $0 \leq \omega \leq \pi$ because we assume in this example that all time domain quantities are real valued. Assume $M = 2$ (two band DMT). The two filters of the PCFB for the above power spectrum are

[2]Readers familiar with singular value decomposition and principal component reconstruction will notice an analogy.

shown in Fig. 17(b), and the traditional brickwall filter bank response is shown in Fig. 17(d). For purpose of calculation assume that the desired probability of error is 10^{-9} in each band and that the number of bits per symbol in the two PAM constellations are $b_0 = 6$ and $b_1 = 2$. If the sampling rate is 2 MHz this implies a bit rate of 8 Mbits/sec. The average power needed can be found from (8). It turns out that the power required by the PCFB is nearly 10 times smaller than the power required by the brickwall filter bank. For example if the brickwall system requires 56 milliwatts, then the PCFB uses only about 5.67 milliwatts for the same performance! For DMT systems with larger number of bands, the difference is less dramatic. In fact for very large M the performances are nearly identical [25].

It turns out that for a monotone decreasing (or increasing) power spectrum the ideal PCFB is precisely the brickwall filter bank. For a power spectrum with many variations, especially bumps and dips as in Fig. 17(a) the PCFB has filters with many passbands and its performance differs significantly from the brickwall filter bank as demonstrated in the preceding example.

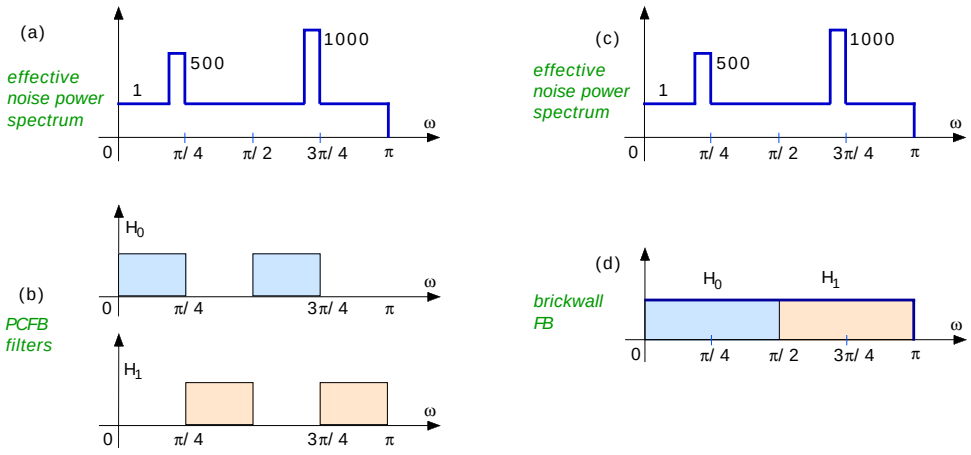

Fig. 17. An example showing the difference between brickwall stacking and PCFB stacking. Here $M = 2$. The PCFB tends to distribute the variances in such a way that one subband variance is maximized and the other is minimized. Each filter in a PCFB can have more than one passband. See text.

A practical example is the effective noise spectrum in a **twisted pair** channel used for ADSL (asymmetric DSL) service. The twisted pair is a pair of insulated copper wires that are twisted at periodic intervals.[3] It reaches every home in the world that has a wireline telephone. The channel gain of the twisted pair decays rapidly with frequency and wirelength. Figure 18 shows a typical qualitative example. The two dips in the figure are created by **bridged taps** which are used in the United States to provide additional service flexibility [18]. Inspite of the large attenuation, it is still possible to use the twisted pair over a large frequency range (up

[3]The idea of twisting originated from Alexander Graham Bell who invented it around 1880, with a view to cancelling the effect of electromagnetic interference.

to a few MHz) and achieve high rates. Several types of DSL services are based on exploiting its bandwidth like this. Originally intended for transmission of baseband speech (about 4 kHz bandwidth) more than 100 years ago, the twisted pair copper wire has therefore come a long way in terms of bandwidth utilization and commercial application. This has given rise to the popular saying that *the DSL technology turns copper into gold.*

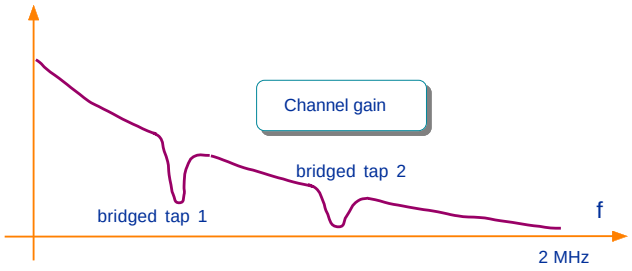

Fig. 18. The channel gain in a twisted pair copper line is a decaying function, with severe attenuation at high frequencies. Moreover, there are sharp dips at various frequencies due to the presence of bridged taps.

It is typical to have 50 twisted pairs bundled into one cable for several kilofeet. As a result, the most dominant noise is the interference created by services from other cables. Two kinds of such interference can be distingushed, namely near end cross talk abbreviated as **NEXT**, and far end cross talk abbreviated as **FEXT**. Essentially, NEXT is the cross-talk from a transmitter at the same side of the cable whereas FEXT is the cross-talk from a transmitter at the other end of the cable. The statistics of these have been studied for many years both theoretically and by extensive measurements [18]. Figure 19 shows typical power spectra of the NEXT and FEXT noise sources in a 50-pair cable. In addition to the NEXT and FEXT, DSL services also suffer from AM radio interference and amateur radio (HAM) interference as shown schematically in the figure. The main point of this discussion is that the total noise spectrum is quite complicated and is far from a constant or a monotone decreasing function. And since the channel gain has dips due to bridge taps, the effective noise spectrum $S_{ee}(e^{j\omega})/|C(e^{j\omega})|^2$ has several bumps and dips. A PCFB is therefore significantly different from the brickwall filter bank. A detailed example presented in [25] for typical ADSL downstream service shows that the difference in performance can be significant for small number of subchannels M. For example, assume $M = 8$ and probability of error 10^{-9} in each subchannel. With typical numbers chosen for various noise components for the ADSL downstream scenario, the required power can be calculated. For an overall bit rate of 3.2 Mb/s it is verified in [25] that the required power is **4.68 mW for traditional DFT** type of multitone, and only **0.94 mW for PCFB** using ideal filters. The intermediate value of 2.76 mW is achieved when traditional DFT is replaced by the KLT. Finally traditional ideal brickwall filter bank uses 1.28 mW,

slightly worse than the ideal PCFB.

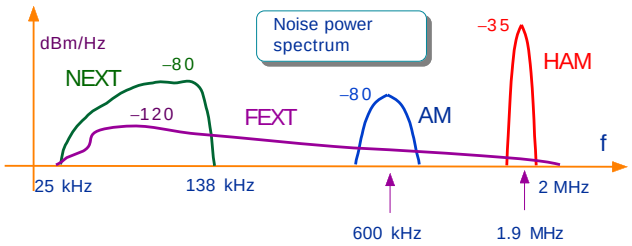

Fig. 19. Various components contributing to the noise spectrum in the ADSL service offered on a twisted pair line. The figure shows the noise power spectra in milliwatts per hertz on a dB scale. The unit dBm stands for $10\log_{10}(\text{mW})$.

11. FILTER BANKS WITH REDUNDANCY

We now mention some generalizations of the DMT structure that have received significant attention recently, especially in the signal processing community. First consider Fig. 20 and compare with the DFT based DMT system of Fig. 14. The DFT and IDFT matrices have been replaced with the matrices $\mathbf{R}(z)$ and $\mathbf{E}(z)$ which can depend on z. This means that the filters $F_k(z)$ and $H_k(z)$ can have arbitrarily large orders. This freedom can be exploited to design DMT systems with better performance (e.g., smaller total power for a given set of requirements).

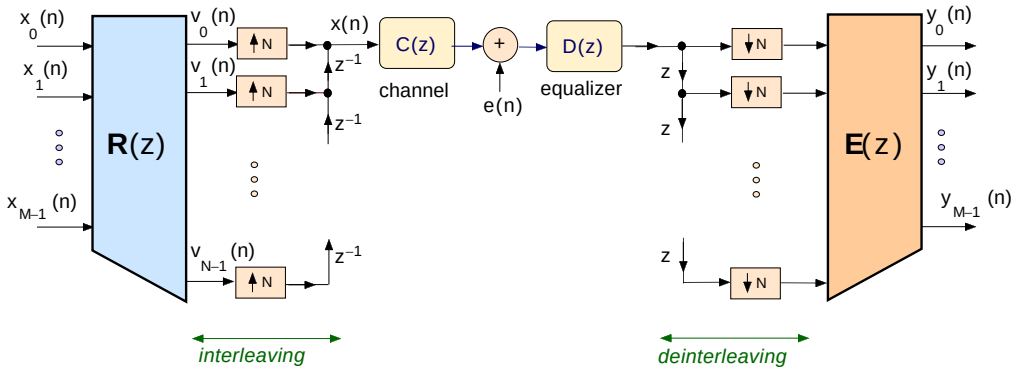

Fig. 20. A DMT system with redundancy.

Second, and more importantly, there is a new integer $N > M$ in the figure which represents the number of outputs of $\mathbf{R}(z)$. The expanders $\uparrow N$ and the set of delay elements following them simply interleave the outputs of $\mathbf{R}(z)$ to produce the composite channel signal $x(n)$ (see Fig. 6(a)). Using standard multirate identities [22] we can draw the system of Fig. 20 in terms of transmitting and receiving filters as shown

in Fig. 21. If the samples of $x_k(n)$ are separated by 1 second, for example, then the samples of $x(n)$ are separated by $1/N$ seconds, instead of $1/M$ seconds as before. This introduces redundancy because the actual symbol rate of M per second has been increased to N per second. The factor N/M is called the *bandwidth expansion factor*.

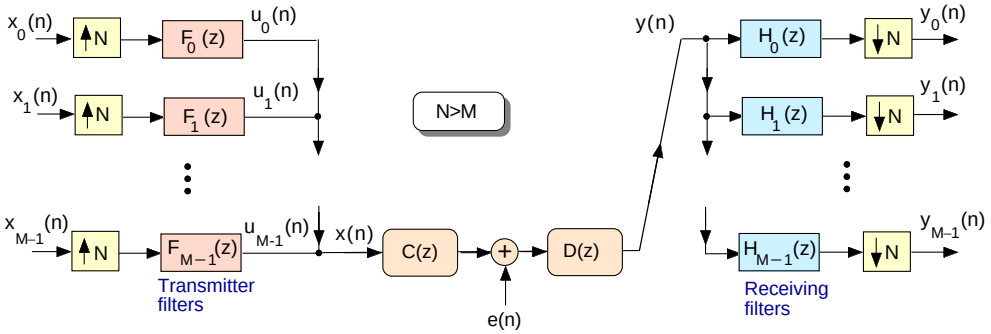

Fig. 21. Redrawing the DMT system with redundancy. The only difference from Fig. 7(a) is that the expander ratio is N which is larger than M.

There are good practical reasons for the incorporation of such redundancy. For example channel equalization is easier [6]; there is no need to directly approximate the channel inverse $1/C(z)$, which is undesirable when $C(z)$ is a filter of high order. In a DMT system with redundancy, it is customary to use a simple FIR or IIR equalizer $D(z)$ such that the product $D(z)C(z)$ is a good approximation of an FIR filter of small length, say L. This is called the **channel shortening** step. Now, if the integer N is chosen as $N = M + L - 1$, we have $L-1$ extra rows in the matrix $\mathbf{R}(z)$. It is possible to choose these appropriately in such a way that a simple set of M multipliers at the output of $\mathbf{E}(z)$ can equalize the channel practically completely. One special case of this idea is where the first M rows of $\mathbf{R}(z)$ are chosen from the DFT matrix and the last $L-1$ rows are repetitions of the first $L-1$ rows. This results in a scheme called the **cyclic prefix** explained in detail in [13]. Further interesting extensions and deeper results can be found in [11].

11.1. Filter Bank Precoders

In a DMT system the symbols $x_k(n)$ are obtained by parsing binary data $s(n)$ as shown earlier in Fig. 8(a). Instead of this, imagine that the symbols $x_k(n)$ are obtained by blocking a scalar signal $s(n)$ which itself belongs to a PAM or QAM constellation. Then the structure of Fig. 20 can be redrawn as in Fig. 22. In this system, a sequence of symbols $s(n)$ is converted to another sequence $x(n)$ before being fed into the channel.

If we assume that two successive samples of $x_k(n)$ are spaced apart by one second, then the samples of $s(n)$ are separated only by $1/M$ seconds and the channel input samples $x(n)$ are separated by the even smaller duration of $1/N$ seconds (see the blue, green and red signals in the figure). This is a way of incorporating

redundancy into a signal before putting it on the channel. The system shown in the figure is called a **filter bank precoder**. By using standard multirate identities, the system of Fig. 22 can be redrawn as shown in Fig. 23(a) or equivalently as in Fig. 23(b).

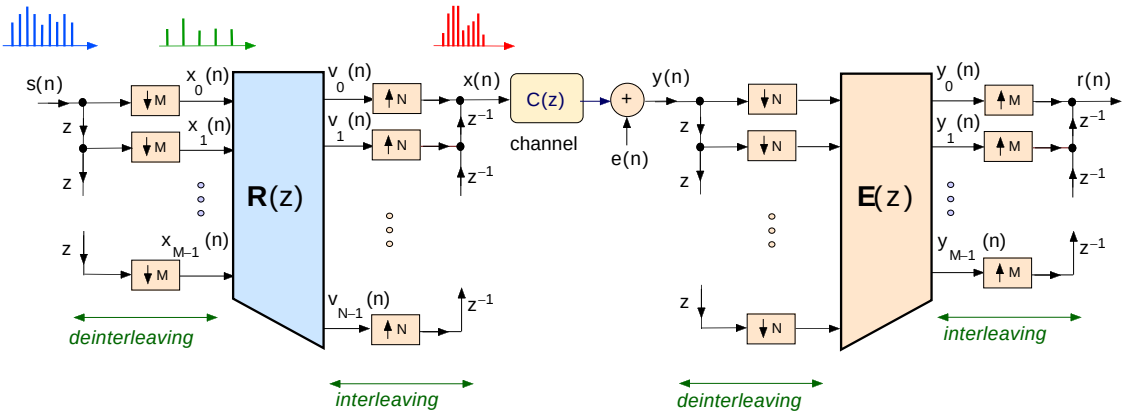

Fig. 22. A modification of the redundant filter bank of Fig. 20. This is called the filter bank precoder. The only conceptual difference is in the interpretation of the vector $\{x_0(n), x_1(n), \ldots x_{M-1}(n)\}$. The precoder allows us to equalize FIR channels with FIR filters. It also opens up the possibility of blind equalization. See text.

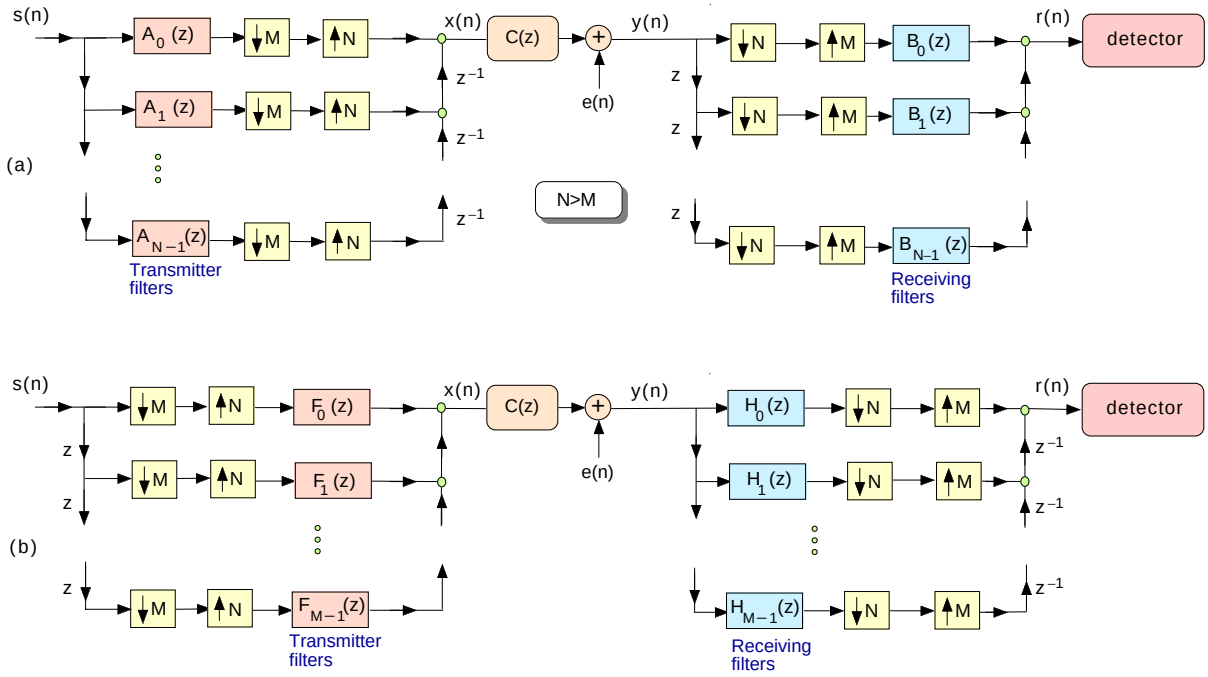

Fig. 23. (a) The filter bank precoder redrawn to show the transmitting and receiving filters. Notice that there are N transmitting filters. (b) An equivalent drawing where the number of filters is M instead of N. Note that the delay and advance operators have been relocated as well. Both configurations have been used in the literature [15], [29].

There are many applications which can be described with the help of the filter bank precoder configuration. If $s(n)$ comes from a finite field and all the arithmetic operations in the filtering are finite field operations, then we can derive traditional channel coders [14] such as **block coders** and **convolutional coders** as special cases of this system. These introduce redundancy in order to make the best use of the noisy channel. A more recent application is the use of such redundancy in **channel equalization**. The channel $C(z)$ can usually be approximated well by an FIR or stable IIR filter. The zero forcing equalizer $1/C(z)$ is in general IIR and could even be unstable (poles outside the unit circle). When we introduce redundancy as above, the use of an IIR filter to approximate $1/C(z)$ is unnecessary. In a beautiful paper [29] Xia has shown that for almost any channel (FIR or IIR) there exist FIR filters $A_k(z)$ and $B_k(z)$ such that the channel is completely equalized (i.e., the received signal $r(n)$ is equal to $s(n)$ in absence of channel noise $e(n)$). In fact the well known class of fractionally spaced equalizers (FSE) [19] is a special case of the filter bank precoder with $M = 1$ and uses N-fold redundancy. The fascinating fact about the filter bank precoder is that even if $M = N - 1$ it is almost always possible to have such FIR equalizers; by making N arbitrarily large we can therefore reduce the bandwidth expansion factor $N/(N-1)$ to almost unity and still have FIR equalization!

All the above discussions assume that the channel transfer function $C(z)$ is known. There are many situations where this is not true. In these cases the removal of intersymbol interference from the received signal falls under the category of **blind equalization**. It has been shown by Giannakis [8] that the redundancy introduced by filter bank precoders can actually be exploited to perform blind equalization. Further detailed results on blind as well as non-blind equalization with filter banks can be found in [15] and [16].

12. CONCLUDING REMARKS

Filter banks have solved a number of problems in communications, but many new questions and ideas have been opened up as well. In Sec. 7 we imposed the perfect symbol recovery condition (or biorthogonality condition) on the DMT filter bank and furthermore assumed a zero forcing equalizer. The filters were optimized under these two conditions. However, neither of these conditions is actually necessary. In fact, apriori imposition of these conditions is a loss of generality. It is more appropriate to optimize the transmitter and receiver filters jointly (the equalizer being regarded as part of the receiver filters). For example we could impose a power constraint and optimize these filters for maximization of signal to noise ratio at the detector input. Some of these ideas have been pursued in the context of filter bank precoders in [15]. A further generalization of the DMT system can be obtained by using nonuniform filter banks (i.e., systems where the decimator and expander are not the same in all bands).

REFERENCES

[1] Akansu, A. N., Duhamel, P., Lin, X., and Courville, M. de. "Orthogonal transmultiplexers in communications: a review," IEEE Trans. SP, April 1998.

[2] Akkarakaran, S., and Vaidyanathan, P. P. "Filter bank optimization with convex objectives, and the optimality of principal component forms," IEEE Trans. SP, pp. 100–114, Jan. 2001.

[3] Akkarakaran, S., and Vaidyanathan, P. P. "Discrete multitone communication with principal component filter banks", Proc. of the ICC, Helsinki, Finland, June 2001.

[4] Bingham, J. A. C. "Multicarrier modulation for data transmission: an idea whose time has come," IEEE Comm. Mag., pp. 5–14, May 1990.

[5] Chow, J. S., Tu, J. C., and Cioffi, J. M. "A discrete multitone transreceiver system for HDSL applications," IEEE J. Selected Areas of Communications, pp. 895–908, Aug., 1991.

[6] Cherubini, G., Eleftheriou, E., Olcer, S., and Cioffi, J. M. "Filter bank modulation techniques for very high speed digital subscriber lines," IEEE Communications Magazine, pp. 98–104, May 2000.

[7] Crochiere, R.E., and Rabiner, L. R. *Multirate digital signal processing,* Prentice Hall, Inc., 1983.

[8] Giannakis, G. B. "Filter banks for blind channel identification and equalization," IEEE Signal Processing Letters, vol. 4, no. 6, pp. 184–187, June 1997.

[9] Kalet, I. "The multitone channel", IEEE Trans. Comm., pp. 119–124, Feb. 1989.

[10] Lin, Y.-P., and Phoong, S.-M., "Perfect discrete multitone modulation with optimal transceivers," IEEE Trans. SP, vol. 48, pp. 1702–1712, June. 2000.

[11] Lin, Y.-P., and Phoong, S.-M., "Minimum redundancy ISI free FIR filter bank transceivers," Proc. of the SPIE, vol. 4119, San Diego, CA, pp. 745–755, July 2000.

[12] Narasimha, M. J., and Peterson, A. M. "Design of a 24-channel transmultiplexer," IEEE Trans. Acoust., Speech, and Signal Proc., vol. 27, Dec. 1979.

[13] Peled, A., and Ruiz, A. "Frequency domain data transmission using reduced computational complexity algorithms," Proc. IEEE ICASSP, pp. 964–967, Denver, CO, April 1980.

[14] Proakis, J. G. *Digital communications,* McGraw Hill 1995.

[15] Scaglione, A., Giannakis, G. B., and Barbarossa, S. "Redundant filter bank precoders and equalizers Part I: Unification and optimal designs", IEEE Trans. Signal Processing, vol. 47, no. 7, pp. 1988-2006, July 1999.

[16] Scaglione, A., Giannakis, G. B., and Barbarossa, S. "Redundant filter bank precoders and equalizers Part II: Synchronization and direct equalization", IEEE Trans. Signal Processing, vol. 47, no. 7, pp. 2007-2022, July 1999.

[17] Shenoi, K. *Digital signal processing in telecommunications,* Prentice Hall, Inc., 1995.

[18] Starr, T., Cioffi, J. M., and Silverman, P. J. *Understanding digital subscriber line technology,* Prentice Hall, Inc., 1999.

[19] Treichler, J. R., Fijalkow, I., and Johnson, C. R., Jr., "Fractionally spaced equalizers: how long should they be?" IEEE Signal Processing Magazine, pp. 65–81, May 1996.

[20] Tsatsanis, M. K., and Giannakis, G. B., "Principal component filter banks for optimal multiresolution analysis," *IEEE Trans. on Signal Proc.,* vol. 43, pp. 1766–1777, Aug. 1995.

[21] Tzannes, M. A., Tzannes, M. C., Proakis, J. G., and Heller, P. N. "DMT systems, DWMT systems, and digital filter banks", Proc. ICC, pp. 311–315, 1994.

[22] Vaidyanathan, P. P. *Multirate systems and filter banks,* Prentice Hall, Inc., 1993.

[23] Vaidyanathan, P. P., Lin, Y-P., Akkarakaran, S., and Phoong, S-M. "Optimalilty of principal component filter banks for discrete multitone communication systems," Proc. IEEE ISCAS, Geneva, May 2000.

[24] Vaidyanathan, P. P., and Akkarakaran, S. "A review of the theory and applications of optimal subband and transform coders," Journal of Applied and Computational Harmonic Analysis, to appear.

[25] Vaidyanathan, P. P., Lin, Y-P., Akkarakaran, S., and Phoong, S-M. "Discrete multitone modulation with principal component filter banks," Technical report, California Institute of Technology, Dec. 2000.

[26] Vetterli, M. "Perfect transmultiplexers," Proc. ICASSP, pp. 2567–2570, 1986.

[27] Vetterli, M., and Kovačević, J. *Wavelets and subband coding,* Prentice Hall, Inc., 1995.

[28] Vrcelj, B., and Vaidyanathan, P. P. "Theory of MIMO biorthogonal partners and their application in channel equalization", Proc. of the ICC, Helsinki, Finland, June 2001.

[29] Xia, X-G. "New precoding for intersymbol interference cancellation using nonmaximally decimated multirate filter banks with ideal FIR equalizers," IEEE Trans. Signal Processing, vol. 45, no. 10, pp. 2431–2441, Oct. 1997.